A Novel Neuromuscular Head-Neck Model and Its Application on Impact Analysis

Zhefen Zheng, Fuhao Mo, *Member, IEEE*, Tang Liu, and Xiaogai Li

***Abstract*— Objective: Neck muscle activation plays an important role in maintaining posture and preventing trauma injuries of the head-neck system, levels of which are primarily controlled by the neural system. Thus, the present study aims to establish and validate a neuromuscular head-neck model as well as to investigate the effects of realistic neural reflex control on head-neck behaviors during impact loading. Methods: The neuromuscular head-neck model was first established based on a musculoskeletal model by including neural reflex control of the vestibular system and proprioceptors. Then, a series of human posture control experiments was implemented and used to validate the model concerning both joint kinematics of the cervical spine and neck muscle activations. Finally, frontal impact experiments of varying loading severities were simulated with the newly established model and compared with an original model to investigate the influences of the implanted neural reflex controllers on head-neck kinematic responses. Results: The simulation results using the present neuromuscular model showed good correlations with in-vivo experimental data while the original model even cannot reach a correct balance status. Furthermore, the vestibular reflex is noted to dominate the muscle activation in less severe impact loadings while both vestibular and proprioceptive controllers have a lot of effect in higher impact loading severity cases. Conclusions: In summary, a novel neuromuscular head-model was established and its application demonstrated the significance of the neural reflex control in predicting in vivo head-neck responses and preventing related injury risk due to impact loading.**

***Index Terms*— Neck, neuromuscular, vestibular, proprioceptor, muscle.**

I. Introduction

MUSCLE support plays a vital role in keeping head posture and preventing trauma injuries under impacts. Neuromuscular feedback control of neck muscles is generally presented in stabilizing the head-neck system in the presence of truck motion and other perturbations. Previous experimental studies have indicated that muscle spindle and vestibular system contribute to head-neck stabilization control [1]–[4]. Thus, integrating reasonable neural control strategies in a musculoskeletal head-neck model is necessary to quantitatively investigate the effects of muscle support on head-neck injuries.

In the recent decade, several human body models have been developed with active muscle control strategies. They are primarily categorized into finite element (FE) models and multibody dynamics (MB) models. Taking the FE models as examples, the SAFER A-HBM developed in the previous studies modeled the human's reflexes mechanism for controlling cervical spine muscle activation [5]–[12]. The THUMS Version 5 included Proportion-Integral-Derivative (PID) based active muscle controllers for all body regions [13]. An angle-based and length-based active muscle controller was implemented in the ViVA OpenHBM [12]. Pre-activation with the OpenSim computed muscle control method and PID-based control strategies were included in the Human Active Lower Limb (HALL) model for lower limbs [14], [15]. Some MB models with muscle control strategies were also developed for investigating active muscle effects during sportive or impact injuries, etc., from 1-pivot models [16]–[19] to detailed subsegments [20]–[25]. Recently, Happee *et al.* [26] developed a multisegment head-neck model incorporating several neural controllers in Matlab programming environment. In our group, Zhang *et al.* [27] developed a framework for the musculoskeletal model to include the proprioceptive reflex loop and ascending signals.

Inspired by all those previous works, the present study aims to develop and validate a neuromuscular head-neck model with crucial neural reflex control factors including vestibular and proprioceptive reflex loop, and quantitatively analyze the effects of these neural feedback control signals on the mechanical behaviors of the head-neck system during impact loading. Then, this neuromuscular head-neck model can be further used for related protective or medical device design and evaluation in the future.

II. Method

A. Neuromuscular Head-Neck Model

Based on an OpenSim head-neck musculoskeletal model by Mortensen *et al.* [28] (referred to as the original model throughout the text), we established a neuromuscular head-neck model by combing it with a neural reflex control

Manuscript received March 20, 2021; revised May 9, 2021; accepted June 7, 2021. Date of publication July 12, 2021; date of current version July 26, 2021. This work was supported in part by the National Natural Science Foundation of China under Grant 51875187, in part by the Hunan Youth Talent Program under Grant 2020RC3016, and in part by the Hunan Provincial Natural Science Foundation of China under Grant 2019JJ40021. *(Corresponding author: Fuhao Mo.)*

This work involved human subjects or animals in its research. Approval of all ethical and experimental procedures and protocols was granted by the Second Xiangya Hospital committee under Approval No 2018-019.

Zhefen Zheng and Fuhao Mo are with the College of Mechanical and Vehicle Engineering, Hunan University, Changsha, Hunan 410082, China (e-mail: fuhaomo@hnu.edu.cn).

Tang Liu is with the Department of Orthopedics, Second Xiangya Hospital of Central South University, Changsha, Hunan 410008, China.

Xiaogai Li is with the Department of Biomedical Engineering and Health Systems, KTH Royal Institute of Technology, SE-141 52 Huddinge, Sweden.

Digital Object Identifier 10.1109/TNSRE.2021.3095624

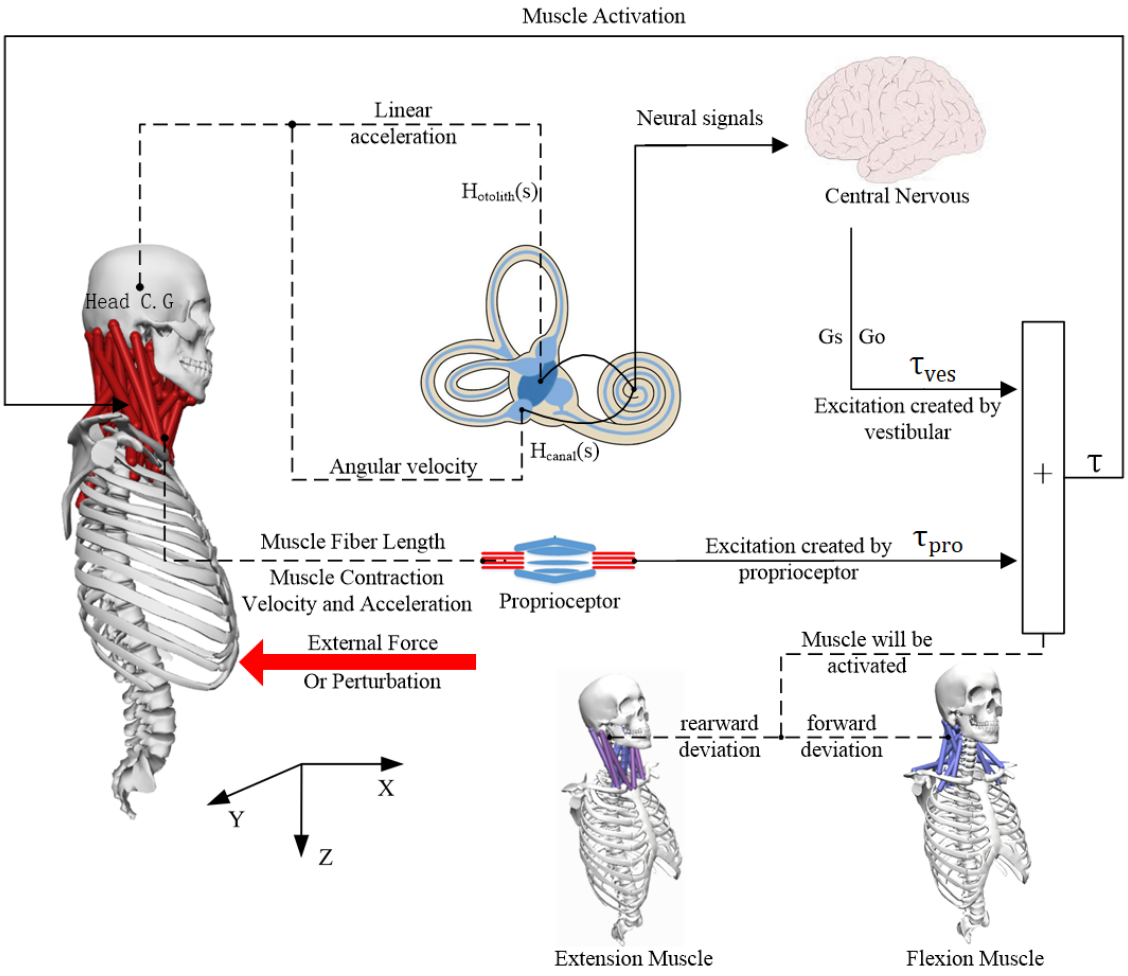

Fig. 1. The schematic of the neuromuscular head-neck model with vestibular and proprioceptive feedback control loops.

strategy programmed in Python codes. The original musculoskeletal model included most of the neck muscles that allow motion in various directions, and approximate passive forces due to ligaments and other structures by setting rotational stiffness and damping between each vertebral joint. The schematic of the control strategy of the neuromuscular head-neck model is shown in Fig. 1. The feedback control loop includes the vestibular reflex that is composed of semicircular canals and otolith organs, and the proprioceptive reflex that is composed of the muscle spindles and Golgi Tendon Organs (GTOs).

When the head or torso is subjected to an external load, the status of the head-neck skeletal system and its supporting muscles change relative to the equilibrium position. The change of head status brings in the feedback neural stimulation signals of the semicircular canal and otolith in the vestibular system, while the change in the supporting muscles leads to the proprioceptive feedback signals in the muscle and tendons. The feedback signals are neural excitations based on the mathematical models of these physiological sensors, which are extracted referring to the angular velocity and linear acceleration of the head, the muscle-tendon length and its contraction velocity, etc. According to previous studies [29]–[31], active movements and different external load would alter the vestibular simuli. In case, two sensitivity parameters of Gs and Go are defined for the semicircular canal feedback and otolith feedback loop, respectively. The neural delays between the vestibular or proprioceptive system and the central nervous system are set to 13ms referring to the previous study [32]. For every timestep, the neural excitations for muscle activations are iteratively calculated by combining the signal of the last timestep and the feedback neural signals due to the current dynamic responses after a defined neural delay. Then, they are transferred to muscle activation levels through activation dynamics. In the present model, the activation dynamics is described as following [33]–[35],

$$\frac{da}{dt} = \frac{u - a}{\tau}$$

where u and a represent the neural spikes and muscle activation, and the τ is the muscle stretch delay. The stretch delay is set to 10 ms for muscle activation and 40 ms for muscle deactivation.

B. Model Feedback Control Loop

1) Vestibular Reflex: The vestibular system is located in the inner ear and consists of the semicircular canals and otolith organs that sense angular and linear motion, respectively. The semicircular canal organs primarily detect head angular

velocity. Based on Schneider et al [31]. study, linearized canal afferent dynamics was selected for its modeling as follows:

$$H_{\text{canal}}(s) = k\frac{s(s+1/\mathrm{T}_1)}{(s+1/\mathrm{T}_c)(s+1/\mathrm{T}_2)}$$

Concerning regular afferents, the parameters of the transfer function are k = 2.83 (spikes/s)/(deg/s), T_1 = 0.0175 s, T_2 = 0.0027 s, and T_c = 5.7 s. When concerning irregular afferents, the parameters of the transfer function are k = 27.09 (spikes/s)/(deg/s), T_1 = 0.03 s, T_2 = 0.0006 s, and T_c = 5.7 s.

The otolith organs primarily sense a gravity-in force resulting from head linear acceleration and head rotation with respect to gravity. Fernandez and Goldberg [36] studied the discharge of peripheral otolith neurons in response to sinusoidal force variations in the squirrel monkey. Both regularly and irregularly discharging neurons were measured. Based on this study, the afferent dynamics of the otolith organs is described as follows:

$$H_{\text{otolith}}(\mathrm{s}) = K_{\mathrm{OTO}}\frac{(1+k_A\tau_A s)}{1+\tau_A s}\frac{(1+k_v(\tau_v s)^{k_v})}{1+\tau_M s}$$

Concerning regular afferents, the parameters of the transfer function are $\mathrm{k_v}$ = 0.188 (spikes/s)/(deg/s), $\mathrm{k_A}$ = 1.12 (spikes/s)/(deg/s), τ_{A} = 69 s, τ_{M} = 16 ms, and $\mathrm{K_{OTO}}$ = 25.6 ips/g. When concerning irregular afferents, the parameters of the transfer function are $\mathrm{k_v}$ = 0.440 (spikes/s)/(deg/s), $\mathrm{k_A}$ = 1.90 (spikes/s)/(deg/s), τ_{A} = 101 s, τ_{M} = 9 ms, and $\mathrm{K_{OTO}}$ = 20.5 ips/g.

2) Proprioceptive Feedback: Muscle spindle and GTOs were modeled following our previous study [27]. The muscle spindle model was simplified based on Mileusnic *et al.* [37] model that simulated the anatomical features of the muscle spindle. The simplified muscle spindle mathematical model with reduced computational cost mainly included the primary afferent firing Ia, which was obtained based on the muscle stretch information. The expression is as follows:

$$\text{Ia Primary afferent} = G * (\frac{T}{Ksr} - (L_{sr}^N - L_{sr}^0))$$

In this equation, K_{sr} is the sensory region's spring constant, L_{sr}^N is the polar region's threshold length, L_{sr}^0 represents the sensory region's rest length, and T represents the muscle fiber tension as previously described in our study [27].

Considering the GTOs as a kind of force-sensitive organ [38], we defined it using a simple linear model as in our previous study:

$$\text{Ib Primary Afferent} = \begin{cases} 0, & F/F_{MVC} < 0.7 \\ p * F/F_{MVC}, & F/F_{\mathrm{MVC}} > 0.7 \end{cases}$$

Here, F_{MVC} is the isometric contraction force, p is the maximum fusimotor frequency and F is the muscle force, respectively.

C. Model Validation

1) Posture Control Experiment: To validate the model and its controlling strategy, we carried out head-neck balance control experiments of three postures: normal sitting, supine and prone. Five male subjects with an average age of 22±1 years old and an average weight of 62.3±3.2 kg were recruited for the experiments. Non-self-reported history of neurological disorders or head-neck injuries were recruited in the volunteers. The study was approved by the Second Xiangya Hospital committee (NO. 2018-019), and informed consent was obtained from the volunteers before the experiments. The experimental setup is shown in Fig. 2. First, a postural calibrator was used to adjust and keep the volunteers' posture as well as relaxing volunteers' muscles before data collection. Then, it was removed just before the experiment. During the experiments, the subjects were required to keep their head stable for 10 s without any external support in three standard postures. In the whole process, the volunteers were also asked to close their eyes and relax their mind to avoid visual effects and feed forward control as possible. X-ray images by the Difinium6000 DR Medical X-ray Transmitter (General Electric Company, USA) were used to record different joint angles of the cervical spine. The Myomuscle (Noraxon, USA) was used to record contact Electromyogram (EMG) signals of the two primary muscles: sternocleidomastoid and splenius capitis. In one posture experiment, every volunteer needs to take one X-ray shoot and repeat four times EMG measurements. Between the two repeat EMG measurement trials, there are at least 5 minutes of rest for the subject to avoid muscle fatigue. A total of 60 tests were conducted.

In addition, to facilitate EMG normalization as well as to confirm correct sensor placement, all subjects performed muscle maximum voluntary contraction (MVC) tests in both flexion and extension directions by pushing their head against the hand of an experimenter. The maximum voluntary contraction test was repeated twice for every subject. Ten minutes of rest was required between the two trials and recorded the EMG signals of each volunteer under the maximum voluntary contraction for the following normalization process.

2) Model-Based Simulation Setup: According to the experimental loading conditions, we first constrained the torso of the musculoskeletal model in six degrees of freedom (Fig. 2). Then, we set the head-neck system to be free and exposed in the gravitational field with a gravity acceleration of 9.8 m/s2 according to the postures. The simulations were implemented using forward dynamics. During the whole simulation process, variations of the joint kinematics of the cervical spine and muscle activations of the head-neck system were obtained and compared with the above-recorded experimental data. In addition, to verify the effects of the neural controllers, the simulation results with the present neuromuscular model were also compared with the original musculoskeletal model without any neural controllers.

3) Comparative Analysis in Impact Loading: To analyze the effects of the neural reflex controllers on head-neck behaviors under impact loading condition, we simulated a series of volunteer frontal impact tests with the accelerations ranging from 2 g to 15 g with different head-neck models including the abovementioned head-neck musculoskeletal model without any neural reflex controllers, the neuromuscular head-neck model only with the proprioceptive controller, and the model

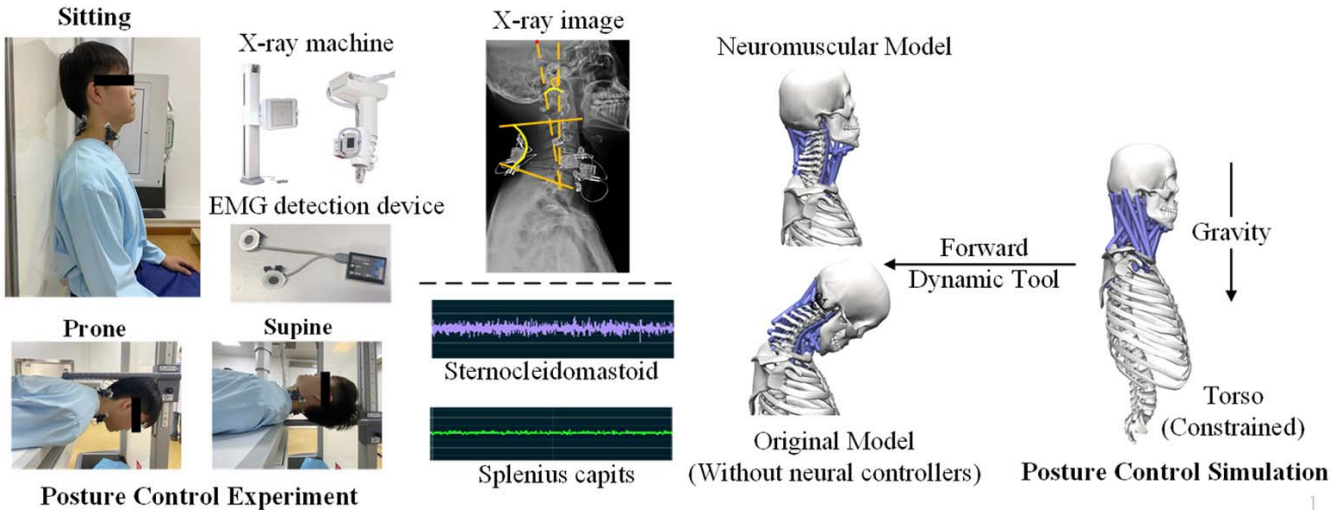

Fig. 2. Posture control experiment setup and its simulation schematic.

with both the vestibular and proprioceptive controllers. Widely referenced frontal impact test data published by National Highway Traffic Safety Administration (NHTSA) were used to evaluate the simulation results [39]. Following the experimental conditions, the external force was applied to the first thoracic vertebra (T1) of the models, and a gravitational field with a gravity acceleration of 9.8 m/s2 was also applied. Different frontal impact severities with volunteer T1 accelerations of 2 g, 3 g, 8 g, and 15 g were simulated. In addition, the pre-activations were also implemented in the head-neck model for considering initial gravity effect in impact analysis based on the simulation results of the sitting posture control. The simulation data in a duration of 350 ms were comparatively analyzed concerning different models and experimental data.

III. Results

A. Experimental Results and Model Validation

Normalized EMG signal corridors of posture control experiments were shown in the Appendix Fig. 7, and cervical joint angles in stable status were listed in the Appendix Table I. The simulation and experimental results of the head-neck posture control in sitting, prone, supine postures are illustrated in Fig. 3. The simulation stabilization processes of different postures are shown in Fig. 3 (a.c.e), while the final joint angles in stable status are shown in the red area of Fig. 3 (b.d.f). The RMS (root mean square) method was used to process the measured raw EMG signals as follows: 1) First, filtering raw EMG signals with a bandpass Butterworth filter at 30-500Hz; 2) Then, the filtered EMG signals were collected by the root mean square using a 20-ms smoothing window; 3) Finally, these signals were normalized by the MVC EMG values to well compare the muscle activations of the posture control experiments with the simulation results. The whole and segmental joint angles of the cervical spine were measured from the X-ray images. The experimental results are presented with grey areas, while the simulation results with the present neuromuscular model and the original musculoskeletal model are presented in solid lines or areas and dash lines or areas, respectively (Fig. 4).

Obviously, faster stabilization processes are noted for the present neuromuscular model in all postures, while the original musculoskeletal model cannot reach a correct equilibrium state even after a long-time balance as shown in Fig. 3 (a, c, e). Concerning both joint angles and muscle activations, the simulation results of the present neuromuscular model reaching the equilibrium state are in good agreement with the experimental data in all three different postures. In the sitting and supine postures, both recorded EMG signals and simulated muscle activations of splenius capitis were close to zero. So, we only compared the activation level of the sternocleidomastoid. As for the prone posture, we only compared the activation level of the splenius capitis. In a further step as shown in Fig. 4 (b, d, f), we note that the detailed segmental joint angles of the cervical spine also correlates well with the X-ray measured corridors. Different sensitive parameter values of the vestibular controller were adopted in the neuromuscular model. In normal siting, the values of Gs and Gc are both 0.65, while for prone and supine postures they both increased to 0.98 and 1.1 for simulating the part of active movement influence on these posture, respectively. All these verified and validated the effectiveness and robustness of our neuromuscular model and its controlling strategy.

B. Effects of Neural Reflex Controllers

A typical comparison of the head-neck kinematics and muscle activations with different simulation models is shown in Fig.4. It is an example of 8g impact loading. Substantial differences in head-neck behaviors and muscle activations can be noted. Following this kinematic comparison, a detailed comparative analysis of the Head C.G Y-rotation displacement vs. Time curves is shown in Fig. 5, which is composed of four impact severity conditions: 2g, 3g, 8g, and 15g impact accelerations. The NBDL experimental corridors

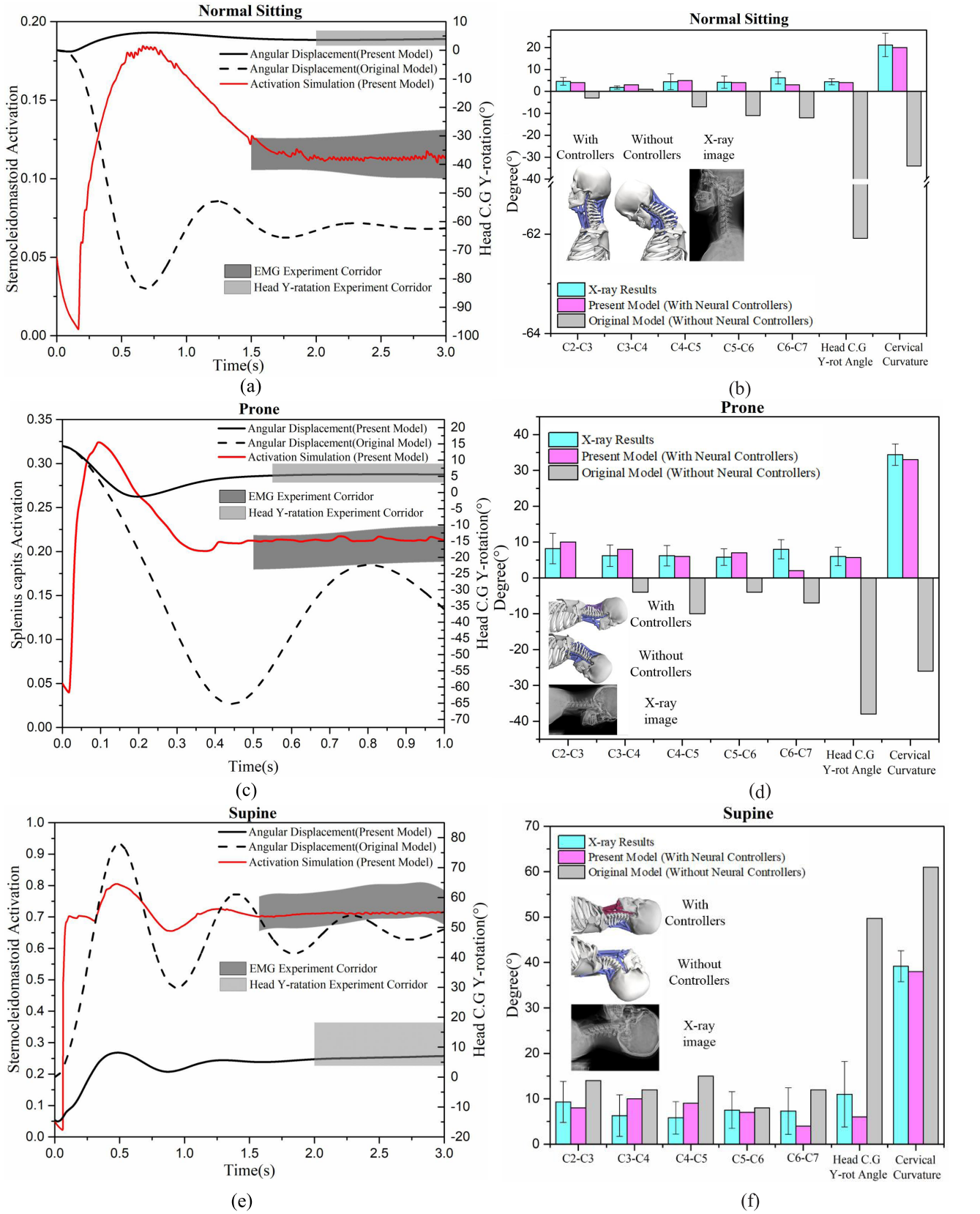

Fig. 3. Model validation and verification in three different postures concerning joint angles and muscle activations: a) Normal Sitting posture, b) Prone posture, c) Supine posture.

are in grey areas, while the averaged curves are in black solid. The simulation curves of the original musculoskeletal model, the neuromuscular model with the only proprioceptive controller, and the neuromuscular model with both vestibular and proprioceptive controllers are illustrated in blue, green and red lines, respectively.

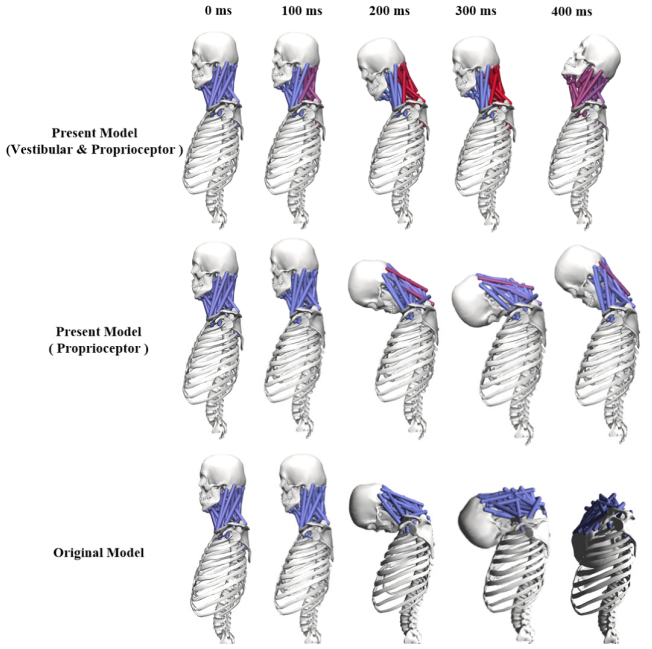

Fig. 4. Typical comparison of head-neck kinematic responses of different models during 8g loading impact.

Obviously, the simulation results of the neuromuscular model with both vestibular and proprioceptive controllers were in better agreement with the experimental corridors in all loading conditions. Especially, those of the passive head-neck model show large deviations with the experimental corridors after the experimental time of the maximum Head C.G Y-rotation. Because the pullback of the head cannot be produced without neural reflex controller in the model. Additionally, we adopted the same vestibular sensitivity parameters (Gs:0.65; Gc:0.65) in 2g and 3g simulation cases. These values were increased to 1.2 for 8g impact loading and 2.4 for 15g impact loading, respectively.

To further investigate neural reflex effects on head-neck kinematics and eliminate the influences of the model passive structure, we compared the primary muscle (splenius capits) activation of different models in the frontal impact loadings as shown in Fig. 6. The solid lines represent the muscle activation levels generated by the neuromuscular model with both vestibular and proprioceptive controllers, and the dashed lines represent the activation levels generated by the neuromuscular model with only proprioceptive controller. The line color represent different impact severity conditions from 2g to 15g.

As shown in both Fig. 5 and Fig. 6, vestibular controller is always noted to play a key role in supporting the head-neck system from low acceleration level of 2g to high acceleration level of 15g. Especially in 2g and 3g loading conditions, it dominates the muscle activations even with smaller values of sensitivity parameters. The proprioceptive controller presents only a minor effect on head-neck responses in 2g and 3g loading conditions but shows a significant effect for higher 8g and 15g loading accelerations, like the vestibular controller.

IV. Discussion

A neuromuscular head-neck model with vestibular and proprioceptive feedback control loops was developed and validated in the present study. We further investigated the influences of these neural reflex controllers on the kinematic responses of the head-neck system in different impact scenarios and verified their significant values in activating neck muscles for supporting the head-neck system and preventing its injuries under excessive external loads. Although the present neuromuscular model can be further improved by including more realistic neural reflex controllers, it is readily applicable for self-balance simulation of the head-neck system and used in various research fields concerning head-neck injury prevention.

Some previous studies investigated the influences of the muscle foreces on head neck injuries, but they generally adopted assumed or PID-based muscle activations [11], [13], [15]. To our knowledge, no study reported the effects of realistic human neural reflex on head-neck impact responses during impact environments. Here, we showed that the muscle support caused by the neural reflex evidently affects impact behaviors of the head-neck system. In this case, we believe that accurate modeling of muscle activation should be accounted for in-vivo head-neck injury analysis. Thus, using cadaver experiments without muscle activation or simulation studies with a passive head-neck model cannot reasonably or robustly capturing in-vivo behaviors of the head-neck system. Even with non-physiological PID or other artificial controllers can not sufficiently reflect a realistic muscle supporting effect. Inspired by these, we believe that more attention should be paid to the modeling of the realistic human neural control strategy.

Although the chosen sensitivity parameters achieved good correlation with experimental data in low impact simulation cases, larger values are needed to achieve better fitting results with the experimental data for higher acceleration loading conditions. The output neural reflex control signal of the vestibular controller is based on the acceleration and the angular velocity of the head [29]. From a physiologic view, adjusting these sensitivity parameters can be rational. An previous study has proposed that the increased variability of firing rate and sensitivity are strongly correlated in the vestibular system [40], which most likely originated from intrinsic properties [41], [42]. This variability might be just a consequence of the increased gain [31]. Because this can prompt the vestibular system to make appropriate adjustments when subjected to different external stimuli to maintain the balance of the head and body [2], [43]. Schneider *et al.* [31] also indicated that an increased sensitivity of the vestibular system optimized human body's coding of external stimuli to maintain head balance. In the future, experimental studies concerning the sensitivity of the vestibular controller can be implemented.

In addition, a slight change of the vestibular sensitivity parameters from 0.98 in prone simulation to 1.1 in supine simulation can be noted. This could be attributed to the feed forward effect of human active movement as mentioned by the previous study [30]. Due to the uncertainty

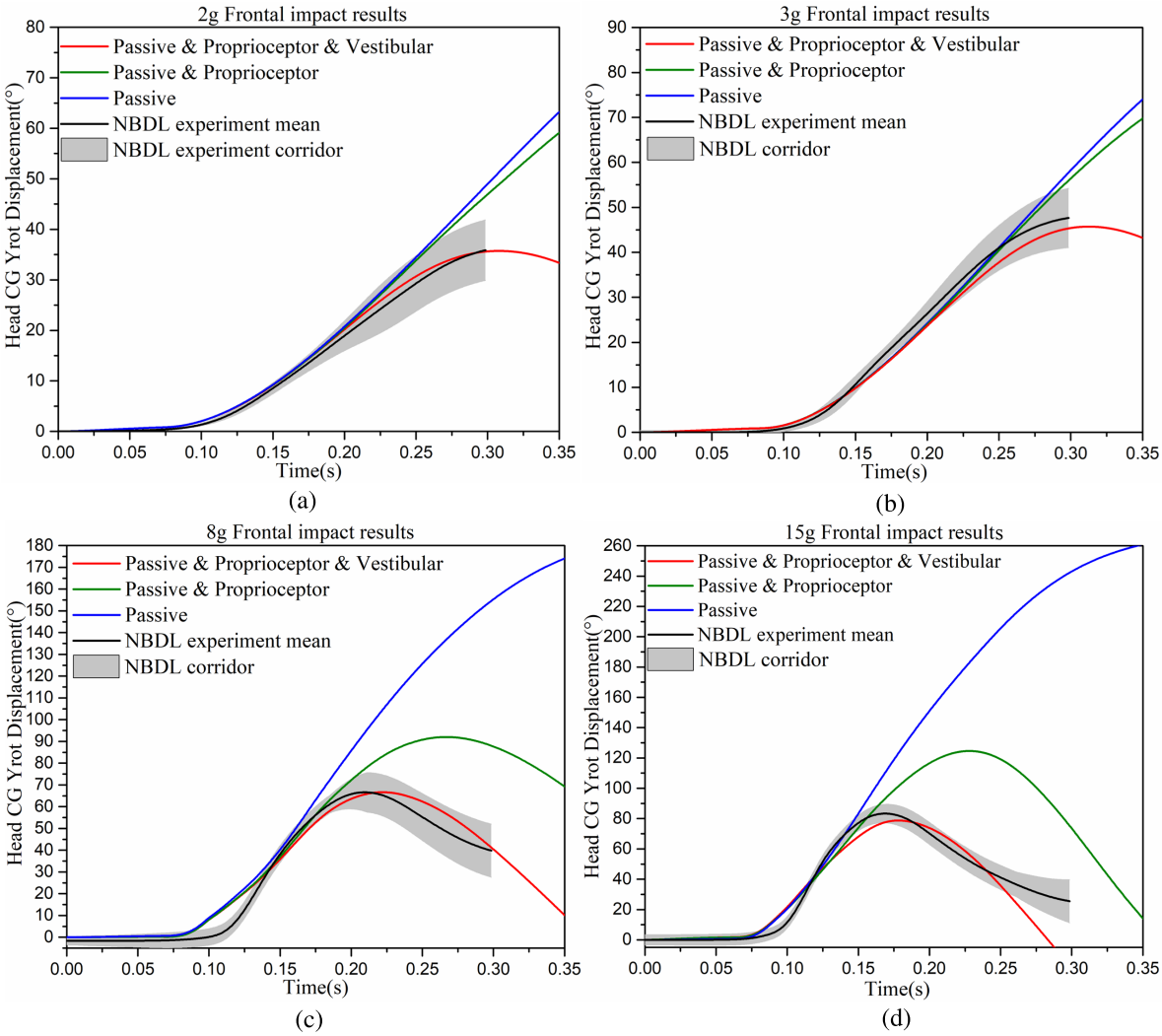

Fig. 5. Effects of neural reflex on head-neck responses during impact loading concerning the Head C.G Y-rotational displacement in relation to T1: a) 2g impact loading; b) 3g impact loading; c) 8g impact loading; d) 15g impact loading.

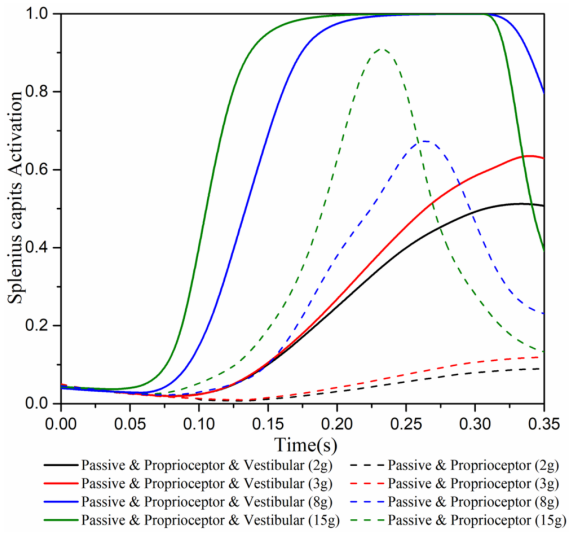

Fig. 6. Effects of neural reflex on muscle activation in different impact loadings.

of the human active movement, there is still not robust method to analyze the influences of feed forward on the head-neck stability. Thus, the present model only included vestibular and proprioceptive controllers, and was used for impact loading analysis. Considering different applications, the present model can be further improved by assign part of the parameters to a certain feedforward influence, or integrating other neural controllers, like visual feedback, central pattern generation, etc.

V. Conclusion

A novel neuromuscular head-neck model including realistic neural reflex control loops of the vestibular system and the muscle-tendon proprioceptors was established and validated in the present study. A series of in-vivo posture control experiments was implemented, and the model validation with the obtained results first proved its self-balance ability in movement control concerning both joint kinematics and muscle activation levels. Then, the models with different neural reflex controllers or without them were used to simulate frontal impact situations. For all impact cases, the present neuromuscular model achieved a good fitting with the experimental results while the model without neural reflex controllers showed a large deviation. We also noted that the vestibular controller dominated the muscle supporting effects

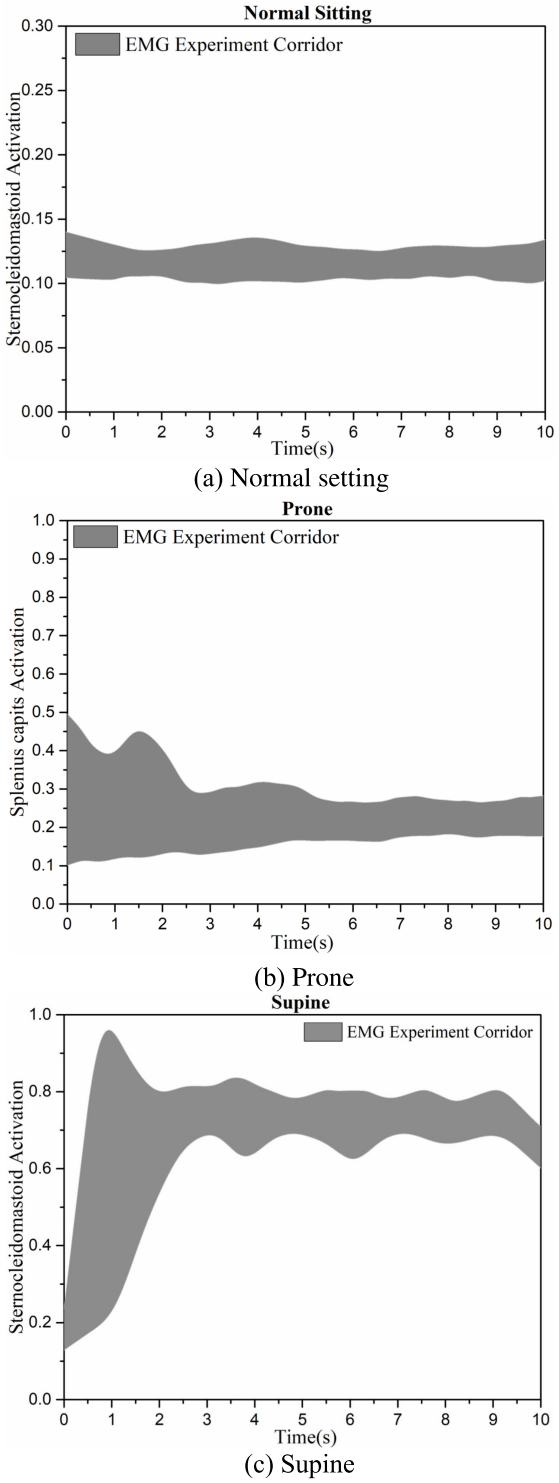

Fig. 7. Normalized EMG signal corridors of posture control experiments.

in lower acceleration loading cases while both vestibular and proprioceptive controllers obviously affected the head-neck behaviors in higher acceleration loading cases. Inspired by all of these, we believe that the accurate modeling of a realistic head-neck neural reflex control strategy plays a key role in predicting in-vivo head-neck behaviors and related injury risk during impact loading.

TABLE I
JOINT ANGLES OF POSTURE CONTROL EXPERIMENTS

Joint	Mean	Standard Deviation (SD)
C2-C3 Normal Sitting (°)	4.6	1.36
C2-C3 Prone (°)	8.2	4.76
C2-C3 Supine (°)	9.3	3.40
C3-C4 Normal Sitting (°)	1.8	0.75
C3-C4 Prone (°)	6.2	2.99
C3-C4 Supine (°)	6.3	3.54
C4-C5 Normal Sitting (°)	4.5	2.06
C4-C5 Prone (°)	6.6	3.07
C4-C5 Supine (°)	5.7	2.32
C5-C6 Normal Sitting (°)	4.2	2.79
C5-C6 Prone (°)	5.8	2.32
C5-C6 Supine (°)	7.5	3.14
C6-C7 Normal Sitting (°)	6.4	5.04
C6-C7 Prone (°)	8.0	2.68
C6-C7 Supine (°)	7.2	3.97
Head Y-rot Angle Normal Sitting (°)	4.2	2.04
Head Y-rot Angle Prone (°)	6.0	2.61
Head Y-rot Angle Supine (°)	11.0	7.20
Cervical Total Angle Normal Sitting (°)	16.4	10.31
Cervical Total Angle Prone (°)	33.2	4.60
Cervical Total Angle Supine (°)	39.2	11.25

CONFLICT OF INTEREST

The authors declared that they have no competing interests in this study.

APPENDIX

See Fig. 7 and Table I.

REFERENCES

[1] P. A. Forbes *et al.*, "Frequency response of vestibular reflexes in neck, back, and lower limb muscles," *J. Neurophysiol.*, vol. 110, no. 8, pp. 1869–1881, Oct. 2013.
[2] P. A. Forbes, G. P. Siegmund, R. Happee, A. C. Schouten, and J.-S. Blouin, "Vestibulocollic reflexes in the absence of head postural control," *J. Neurophysiol.*, vol. 112, no. 7, pp. 1692–1702, Oct. 2014.
[3] J. M. Goldberg and K. E. Cullen, "Vestibular control of the head: Possible functions of the vestibulocollic reflex," *Exp. Brain Res.*, vol. 210, nos. 3–4, pp. 331–345, May 2011.
[4] G. C. Y. Peng, T. C. Hain, and B. W. Peterson, "Predicting vestibular, proprioceptive, and biomechanical control strategies in normal and pathological head movements," *IEEE Trans. Biomed. Eng.*, vol. 46, no. 11, pp. 1269–1280, Nov. 1999.
[5] M. A. Correia, S. D. McLachlin, and D. S. Cronin, "Optimization of muscle activation schemes in a finite element neck model simulating volunteer frontal impact scenarios," *J. Biomech.*, vol. 104, May 2020, Art. no. 109754.

[6] C. Dehner, S. Schick, M. Kraus, A. Scola, W. Hell, and M. Kramer, "Muscle activity influence on the kinematics of the cervical spine in frontal tests," *Traffic Injury Prevention*, vol. 14, no. 6, pp. 607–613, 2013.

[7] X. Jin, Z. Feng, V. Mika, H. Li, D. C. Viano, and K. H. Yang, "The role of neck muscle activities on the risk of mild traumatic brain injury in American football," *J. Biomech. Eng.*, vol. 139, no. 10, Oct. 2017, Art. no. 101002.

[8] J. Östh, K. Brolin, and D. Bråse, "A human body model with active muscles for simulation of pretensioned restraints in autonomous braking interventions," *Traffic Injury Prevention*, vol. 16, pp. 304–313, Apr. 2015.

[9] J. Osth, K. Brolin, S. Carlsson, J. Wismans, and J. Davidsson, "The occupant response to autonomous braking: A modeling approach that accounts for active musculature," *Traffic Injury Prevention*, vol. 13, no. 3, pp. 265–277, 2012.

[10] J. Osth, K. Brolin, and R. Happee, "Active muscle response using feedback control of a finite element human arm model," *Comput. Methods Biomech. Biomed. Eng.*, vol. 15, no. 4, pp. 347–361, 2012.

[11] J. Osth, M. Mendoza-Vazquez, F. Sato, M. Y. Svensson, A. Linder, and K. Brolin, "A female head-neck model for rear impact simulations," *J. Biomech.*, vol. 51, pp. 49–56, Jan. 2017.

[12] I. P. A. Putra, J. Iraeus, F. Sato, M. Y. Svensson, A. Linder, and R. Thomson, "Optimization of female head-neck model with active reflexive cervical muscles in low severity rear impact collisions," *Ann. Biomed. Eng.*, vol. 49, no. 1, pp. 115–128, Jan. 2021.

[13] M. Iwamoto, Y. Nakahira, and D. Kato, "Finite element analysis for investigating the effects of muscle activation on head-neck injury risks of drivers rear-ended by a car after an autonomous emergency braking," *Int. J. Automot. Eng.*, vol. 9, no. 3, pp. 124–129, 2018.

[14] F. Mo, F. Li, M. Behr, Z. Xiao, G. Zhang, and X. Du, "A lower limb-pelvis finite element model with 3D active muscles," *Ann. Biomed. Eng.*, vol. 46, no. 1, pp. 86–96, Jan. 2018.

[15] F. Mo, J. Li, M. Dan, T. Liu, and M. Behr, "Implementation of controlling strategy in a biomechanical lower limb model with active muscles for coupling multibody dynamics and finite element analysis," *J. Biomech.*, vol. 91, pp. 51–60, Jun. 2019.

[16] M. A. Fard, T. Ishihara, and H. Inooka, "Dynamics of the head-neck complex in response to the trunk horizontal vibration: Modeling and identification," *J. Biomech. Eng.*, vol. 125, no. 4, pp. 533–539, Aug. 2003.

[17] G. C. Y. Peng, T. C. Hain, and B. W. Peterson, "How is the head held up? Modeling mechanisms for head stability in the sagittal plane," in *Proc. 18th Annu. Int. Conf. IEEE Eng. Med. Biol. Soc.*, vol. 2, Oct./Nov. 1997, pp. 627–628.

[18] S. Rahmatalla and Y. Liu, "An active head-neck model in whole-body vibration: Vibration magnitude and softening," *J. Biomech.*, vol. 45, no. 6, pp. 925–930, Apr. 2012.

[19] Y. Wang and S. Rahmatalla, "Human head-neck models in whole-body vibration: Effect of posture," *J. Biomech.*, vol. 46, no. 4, pp. 702–710, Feb. 2013.

[20] J. Almeida, F. Fraga, M. Silva, and L. Silva-Carvalho, "Feedback control of the head-neck complex for nonimpact scenarios using multibody dynamics," *Multibody Syst. Dyn.*, vol. 21, no. 4, pp. 395–416, 2009.

[21] K. Brolin, S. Hedenstierna, P. Halldin, C. Bass, and N. Alem, "The importance of muscle tension on the outcome of impacts with a major vertical component," *Int. J. Crashworthiness*, vol. 13, no. 5, pp. 487–498, Sep. 2008.

[22] C. Kuo, J. Sheffels, M. Fanton, I. B. Yu, R. Hamalainen, and D. Camarillo, "Passive cervical spine ligaments provide stability during head impacts," *J. Roy. Soc. Interface*, vol. 16, no. 154, May 2019, Art. no. 20190086.

[23] B. D. Stemper, N. Yoganandan, and F. A. Pintar, "Validation of a head-neck computer model for whiplash simulation," *Med. Biol. Eng. Comput.*, vol. 42, no. 3, pp. 333–338, May 2004.

[24] A. Wittek, J. Kajzer, and E. Haug, "Hill-type muscle model for analysis of mechanical effect of muscle tension on the human body response in a car collision using an explicit finite element code," *JSME Int. J. A*, vol. 43, no. 1, pp. 8–18, 2000.

[25] N. Yoganandan, F. A. Pintar, and J. F. Cusick, "Biomechanical analyses of whiplash injuries using an experimental model," *Accident Anal. Prevention*, vol. 34, no. 5, pp. 663–671, 2002.

[26] R. Happee, E. de Bruijn, P. A. Forbes, and F. C. T. van der Helm, "Dynamic head-neck stabilization and modulation with perturbation bandwidth investigated using a multisegment neuromuscular model," *J. Biomech.*, vol. 58, pp. 203–211, Jun. 2017.

[27] H. Zhang, F. Mo, L. Wang, M. Behr, and P. J. Arnoux, "A framework of a lower limb musculoskeletal model with implemented natural proprioceptive feedback and its progressive evaluation," *IEEE Trans. Neural Syst. Rehabil. Eng.*, vol. 28, no. 8, pp. 1866–1875, Aug. 2020.

[28] J. D. Mortensen, A. N. Vasavada, and A. S. Merryweather, "The inclusion of hyoid muscles improve moment generating capacity and dynamic simulations in musculoskeletal models of the head and neck," *PLoS ONE*, vol. 13, no. 6, 2018, Art. no. e0199912.

[29] C. Lopez-Vaamonde, J. W. Koning, R. M. Brown, W. C. Jordan, and A. F. Bourke, "Neurons compute internal modelsof the physical laws of motion," *Nature*, vol. 430, no. 6999, pp. 557–560, Jul. 2004.

[30] J. Carriot, M. Jamali, M. J. Chacron, and K. E. Cullen, "Statistics of the vestibular input experienced during natural self-motion: Implications for neural processing," *J. Neurosci., Off. J. Soc. Neurosci.*, vol. 34, no. 24, pp. 8347–8357, Jun. 2014.

[31] A. D. Schneider, M. Jamali, J. Carriot, M. J. Chacron, and K. E. Cullen, "The increased sensitivity of irregular peripheral canal and otolith vestibular afferents optimizes their encoding of natural stimuli," *J. Neurosci., Off. J. Soc. Neurosci.*, vol. 35, no. 14, pp. 5522–5536, Apr. 2015.

[32] P. A. Forbes, E. de Bruijn, A. C. Schouten, F. C. van der Helm, and R. Happee, "Dependency of human neck reflex responses on the bandwidth of pseudorandom anterior-posterior torso perturbations," *Exp. Brain Res.*, vol. 226, no. 1, pp. 1–14, Apr. 2013.

[33] I. Williams and T. G. Constandinou, "Computationally efficient modeling of proprioceptive signals in the upper limb for prostheses: A simulation study," *Frontiers Neurosci.*, vol. 8, p. 181, Jun. 2014.

[34] D. G. Thelen and F. C. Anderson, "Using computed muscle control to generate forward dynamic simulations of human walking from experimental data," *J. Biomech.*, vol. 39, no. 6, pp. 1107–1115, 2006.

[35] S. L. Delp *et al.*, "OpenSim: Open-source software to create and analyze dynamic simulations of movement," *IEEE Trans. Biomed. Eng.*, vol. 54, no. 11, pp. 1940–1950, Nov. 2007.

[36] C. Fernandez and J. M. Goldberg, "Physiology of peripheral neurons innervating otolith organs of the squirrel monkey. I. Response to static tilts and to long-duration centrifugal force," *J. Neurophysiol.*, vol. 39, no. 5, pp. 970–984, Sep. 1976.

[37] M. P. Mileusnic, I. E. Brown, N. Lan, and G. E. Loeb, "Mathematical models of proprioceptors. I. Control and transduction in the muscle spindle," *J. Neurophysiol.*, vol. 96, no. 4, pp. 1772–1788, Oct. 2006.

[38] S. Li *et al.*, "Coordinated alpha and gamma control of muscles and spindles in movement and posture," *Front Comput Neurosci*, vol. 9, p. 122, Oct. 2015.

[39] National Highway Traffic Safety Administration. (2012). *NBDL Human Volunteer Sled Tests Without Car Body 1522 to 1651*. [Online]. Available: https://www-nrd.nhtsa.dot.gov/database/VSR/bio/QueryTest.aspx

[40] M. Jamali, J. Carriot, M. J. Chacron, and K. E. Cullen, "Strong correlations between sensitivity and variability give rise to constant discrimination thresholds across the otolith afferent population," *J. Neurosci., Off. J. Soc. Neurosci.*, vol. 33, no. 27, pp. 11302–11313, Jul. 2013.

[41] C. E. Smith and J. M. Goldberg, "A stochastic afterhyperpolarization model of repetitive activity in vestibular afferents," *Biol. Cybern.*, vol. 54, no. 1, pp. 41–51, May 1986.

[42] R. Kalluri, J. Xue, and R. A. Eatock, "Ion channels set spike timing regularity of mammalian vestibular afferent neurons," *J. Neurophysiol.*, vol. 104, no. 4, pp. 2034–2051, Oct. 2010.

[43] F. A. Keshner and B. W. Peterson, "Mechanisms controlling human head stabilization. I. Head-neck dynamics during random rotations in the horizontal plane," *J. Neurophysiol.*, vol. 73, no. 6, pp. 2293–2301, Jun. 1995.